Advances in Nano Research, *Vol. 13, No. 1 (2022) 87-96*
https://doi.org/10.12989/anr.2022.13.1.087

FA/Mel@ZnO nanoparticles as drug self-delivery systems for RPE protection against oxidative stress

Caixia Yi[1†], Zhihai Yu[2†], Xin Sun[1], Xi Zheng[1], Shuangya Yang[1], Hengchuan Liu[2], Yi Song[*3] and Xiao Huang[**1,4]

[1]*School of Sports and Health Science, Tongren University, Tongren 554300, P. R. China*
[2]*Department of Urology, Chongqing University Three Gorges Hospital, Chongqing 404000, P. R. China*
[3]*Department of Neurosurgery, Chongqing University Three Gorges Hospital, Chongqing 404000, China*
[4]*School of Physical Education, Guangxi University of Science and Technology, Liuzhou 545006, China*

(*Received September 7, 2021, Revised April 14, 2022, Accepted May 15, 2022*)

Abstract. Drug self-delivery systems can easily realize combination drug therapy and avoid carrier-induced toxicity and immunogenicity because they do not need non-therapeutic carrier materials. So, designing appropriate drug self-delivery systems for specific diseases can settle most of the problems existing in traditional drug delivery systems. Retinal pigment epithelium is very important for the homeostasis of retina. However, it is vulnerable to oxidative damage and difficult to repair. Worse still, the antioxidants can hardly reach the retina by non-invasive administration routes due to the ocular barriers. Herein, the targeted group (folic acid) and antioxidant (melatonin) have been grafted on the surface of ZnO quantum dots to fabricate a new kind of drug self-delivery systems as a protectant via eyedrops. In this study, the negative nanoparticles with size ranging in 4~6 nm were successfully synthesized. They could easily and precisely deliver drugs to retinal pigment epithelium via eyedrops. And they realized acid degradation to controlled release of melatonin and zinc in retinal pigment epithelium cells. Consequently, the structure of retinal pigment epithelium cells were stabilized according to the expression of ZO-1 and β-catenin. Moreover, the antioxidant capacity of retinal pigment epithelium were enhanced both in health mice and photic injury mice. Therefore, such new drug self-delivery systems have great potential both in prevention and treatment of oxidative damage induced retinal diseases.

Keywords: antioxidation; combination drug therapy; drug self-delivery system; retinal pigment epithelium; zinc oxide

1. Introduction

The drug delivery systems (DDS) can increase safety, improve stability and enhance bio-availability of the drugs in order to heighten the curative effect and reduce side effects (Yu *et al*. 2020). In order to enhance permeability and retention (EPR) effect and reduce renal clearance, the majority of DDS are prepared at nanoscale (Liu *et al*. 2019, Javadi and Ardestani 2020, Mu *et al*. 2020).

However, a recent study showed that only 0.7% (median) of the administered nanoparticles could reach the targeted site and most of the nanoparticles accumulated in healthy tissues (Wilhelm *et al*. 2016). Furthermore, the drug loading capacity of nanocarriers is usually limited by the material properties (Subrizi *et al*. 2019). As a result, it has to increase the dosage of those DDS to ensure their therapeutic effectiveness. This means that the carrier materials which is lacking of therapeutic activity excessively enter human body. That could be a safety concern. Particularly, the nano-carriers that are not fully metabolised and eliminated would have toxic effects. Moreover, a mass of foreign materials coming into the human body could activate the immune system, potentially leading to immunotoxicity (Piscatelli *et al*. 2021, Ilinskaya *et al*. 2015). These drawbacks have actuated the development of drug self-delivery systems (DSDS). DSDS are pure carrier-free systems. No additional non-therapeutic carrier material is required and the carrier material itself is the drug for the treatment of disease (Qin *et al*. 2017, Shen *et al*. 2017). DSDS are easily to achieve nearly 100% of drug loading capacity and carry out combination drug therapy. In addition, carrier-induced toxicity and immunogenicity can be avoided. Therefore, the development of appropriate DSDS for specific diseases can settle most of the problems existing in traditional DDS.

Retinal pigment epithelium (RPE) is a layer of epithelial cells containing pigment locating between neural retina and choroid. RPE is very important for the homeostasis of retina. However, RPE cells are relatively easily apoptosed induced by oxidative stress. Even worse, RPE cells have limited ability to regenerate if destroyed (Rzhanova *et al*. 2020). Consequently, protecting RPE from injury is essential to maintain the homeostasis of retina. In clinic, giving protectants to prevent RPE against oxidative stress is the common treatment method. Recent studies have shown that zinc (Zn) can be involved in the maintenance of antioxidant status of RPE (Saito *et al*. 2018, Rodriguez-Menendez *et al*. 2018, Alvarez-Barrios *et al*. 2021). Zn binding metallothioneins act as an effective redox system to

*Corresponding author, Professor,
E-mail: soup6@163.com
**Co-corresponding author, Professor,
E-mail: humphrey8531@hotmail.com
†Authors contribute equally to this work

ISSN: 2287-237X (Print), 2287-2388 (Online)

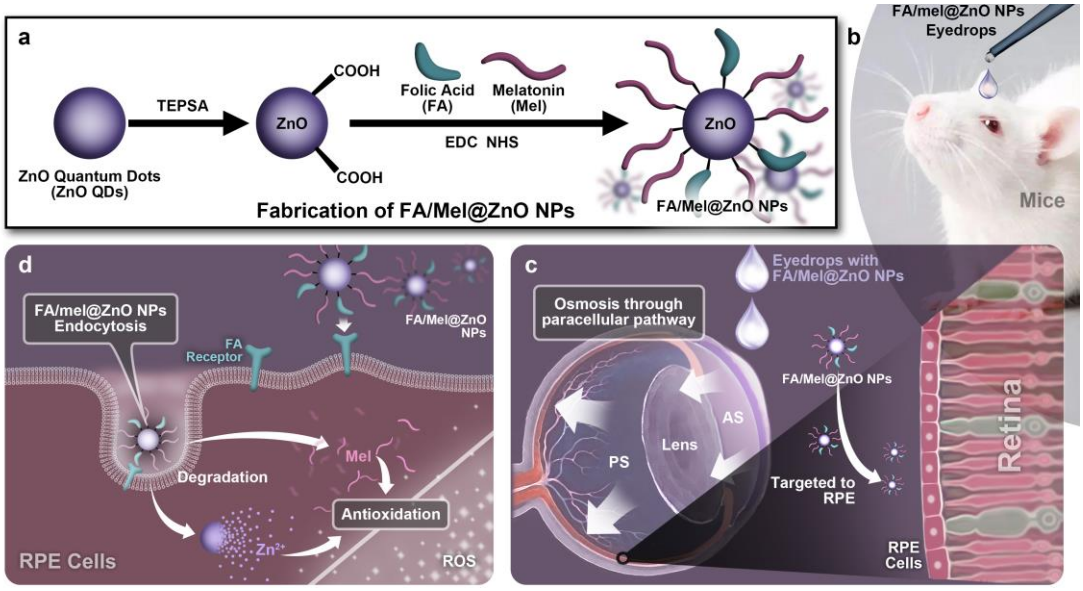

Scheme 1 Schematic diagram of synthesis of FA/Mel@ZnO NPs as well as their delivery and release behavior. Mel and FA were grafted on the surface of ZnO QDs to fabricate smart DSDS (a); FA/Mel@ZnO NPs were administrated via eyedrops (b); which precisely delivered drugs to RPE cells through paracellular pathway (c); The Mel and Zn^{2+} was controlled released in endosome acid environment to cells for combined treatment (d)

scavenge free radicals. Besides, melatonin (Mel) has been also reported to have multiple protective effects on RPE cells against oxidative damage (Chang *et al*. 2018, Mehrzadi *et al*. 2020, Diéguez *et al*. 2020). Regrettably, eyedrop is hardly to deliver drugs to posterior segment and this is similar for systemic administration due to its scarce vascularity. Intravitreal injection holds a low acceptance and is likely to cause infection (Baumal *et al*. 2020). Hence, the obstacle is how to expediently deliver Zn and Mel targeted to RPE for combination protection.

It has been proven that nanoparticles with the size smaller than 6 nm can reach RPE through the conjunctiva and choroid by a paracellular pathway with relative ease (Horibe *et al*. 1997). The size of zinc oxide nanoparticles (ZnO NPs) is controllable and can be smaller than 6 nm (Singh *et al*. 2020). And they can be easily modified to make drug-loading vehicles (Huang *et al*. 2019). Moreover, ZnO rapidly degrade to Zn^{2+} at pH<5.5 which could be Zn source when ZnO NPs enter the cell (Huang *et al*. 2017). These dramatic properties enable ZnO to regard as the reasonable choice for constructing DSDS. Herein, Mel and folic acid (FA, targeting to RPE cells) have been grafted on the surface of ZnO nanoparticles (FA/Mel@ZnO NPs) to fabricate smart DSDS. These DSDS are intended to specifically deliver Mel and Zn to RPE and simultaneously release drugs in RPE cells as a protectant against oxidative stress (Scheme 1).

2. Materials and methods

2.1 Materials

ZnO QDs were a valuable gift from Prof. Yue Wang from China Pharmaceutical University. 3-(Triethoxysilyl) propvlsuccinc anhydride (TEPSA, 95%) was bought from Macklin (China). 1-(3-Dimethylaminopropyl)-3-ethylcarbo diimide hydrochloride (EDC, RG), N-hydroxy succinimide (NHS, RG), FA (RG), and Mel (RG) were purchased from Adamas-beta (China). Compound tropicamide eyedrops were obtained from Santen (Japan). The RPE cell line (ARPE-19) were purchased from ATCC (USA). Dulbecco's modified eagle medium (high glucose) (DMEM), pancreatin, penicillin and streptomycin (PS), and fetal bovine serum (FBS) were obtained from Gibco (USA). Cell counting kit-8 (CCK-8) was obtained from Dojindo (Japan). 1,1'-Dioctadecyl-3,3,3',3'-tetramethylindodicarbo cyanine perchlorate (DID, ≥98.0%) was bought from Sigma-Aldrich (USA). 4',6-Diamidino-2-phenylindole dihydrochloride (DAPI, >90%) was purchased from Soalrbio (China). Reactive oxygen species (ROS) assay kit (DCFH-DA method), lipid peroxidation assay kit (MDA), cellular glutathione peroxidase assay kit (GSH-PX, NADPH method), and total antioxidant capacity assay kit (T-AOC, rapid ABTS method) were purchased from Beyotime (China). Antibodies against zonula occludens-1 (ZO-1), β-catenin, extracellular regulated protein kinases 1/2 (ERK1/2), nuclear factor-erythroid 2-related factor 2 (Nrf2), and glyceraldehyde-3-phosphate dehydrogenase (GAPDH) were bought from Abcam (UK). C57 mouse were purchased from SJA (China).

2.2 Synthesis of carboxyl surface-functionalized ZnO QDs (COOH@ZnO QDs)

50.00 mg of Zn QDs were dispersed in 5 mL of ethanol and kept stirring at 50 ℃. Then 93.37 mg of TEPSA was dropwise added in. The mixture was kept stirring at 50 ℃ for 7 h. After the reaction completed, precipitate was collected by centrifugation and washed trice with ethanol. The production was dried in vacuum, followed by dispersing in deionized water at 80 ℃ for 2 h. The obtained white suspension was collected and dried.

2.3 Mel and FA loading (FA/Mel@ZnO NPs)

20.00 mg of COOH@ZnO QDs were dispersed in 5 mL of deionized water containing 32.86 mg of EDC and stirred for 1 h. 19.70 mg of NHS was added in and the mixture was stirred for another 10 h. Then 11.34 mg of FA and 34.28 mg of Mel was added in and kept stirring for 12 h. The production was collected by centrifugation and washed trice with ethanol.

2.4 Characterization

The content of Zn in COOH@ZnO QDs was detected by a zinc tester. The fourier transform infrared spectrometer (FTIR) spectra of COOH@ZnO QDs and FA/Mel@ZnO NPs were determined by fourier transform infrared spectrometer (Spectrum GX Perkin Elmer, USA). The morphology of ZnO QDs and FA/Mel@ZnO NPs was observed by TEM (FEI Tecnai F20 S-Twin, USA). Their zeta potentials were tested by DLS (Zetasizer Nano S90 Malven, UK). The themogravimetric analysis (TA) of FA/Mel@ZnO NPs was carried out by a simultaneous thermal analyzer with the heating rate of 20 ℃/min (Q600 TA instrument, USA).

2.5 Cell culture

ARPE-19 cells were maintained in DMEM medium supplemented with 10% FBS and 1% PS. ARPE-19 cells were cultured at 37 ℃ in a humidified incubator with 5% CO_2. All cells in exponential growth phase were used for experiments.

2.6 Cytotoxicity

ARPE-19 cells were seeded into 96-well plates with 5000 cells per well. After 12 h, FA/Mel@ZnO NPs solution in different concentrations (10, 20, 40, 80, 100 μM) were added into the medium. Cellular viability was measured using CCK-8 assay after successive cultivation for 24 h under humidified atmosphere. ARPE-19 cells without any treatment were used as positive control to fix the cellular viability as 100%.

2.7 Topical instillation

10 μL of FA/Mel@ZnO NPs solution (1 mg/mL) was dropped into the eye of an eight weeks old female C57 mice. 10 min later, the mice were killed and eyes were removed. The eyes samples were fixed. After dewatering, the samples were embedded in paraffin. Then, the tissues were cut to slices and photographed with a fluorescent microscope. ZnO QDs solution instillation experimental group was set as positive control. Eyes without any treatment experimental group was set as negative control.

2.8 Targeting property of FA/Mel@ZnO NPs to ARPE-19 cells

2×10^4 of ARPE-19 cells were seeded on a coverslip which placed in the well of a 24-well plate. After 12 h, the cell culture medium was drawn out and replaced by fresh medium containing FA/Mel@ZnO NPs at the concentration of 50 μM. Cells were incubated for another 10 min. Then culture medium was drawn out. Cells were vigorously washed with PBS for 3 times and stained using DID for 15 min. After washing with PBS thrice, cells were fixed with 4% paraformaldehyde for 15 min, followed by washing with PBS thrice. Then, cells were stained using DAPI for 10 min. Another three times washing with PBS have been carried out for cells, and the coverslip was taken out and put on a microslide to be observed under a confocal laser scanning microscope (SP8 Leica, Germany). ARPE-19 cells treated with ZnO QDs were set as a control to verify the targeting property of FA combining to folate receptor.

2.9 In vitro drugs release behavior

The drug release behavior was investigated at 37 ℃ in two different media: (a) acetate buffer (pH=5.5); (b) neutral buffer (pH=7.4), using a dialysis bag diffusion technique. 4.80 mg of FA/Mel@ZnO NPs was dispersed in 2 mL of different PBS and sealed in a dialysis bag (MW: 3000 Da). The dialysis bag was submerged in 30 mL of respective PBS and stirred at 37 ℃ for 24 h. The release Mel and Zn was collected at predetermined time points. Mel was analyzed by a UV/Vis spectroscopy. Zn was determined by a zinc tester.

2.10 Endocytosis of FA/Mel@ZnO NPs

2×10^4 of ARPE-19 cells were seeded on a coverslip which placed in the well of a 24-well plate. After 12 h, the cell culture medium was drawn out and replaced by fresh medium containing FA/Mel@ZnO NPs at the concentration of 50 μM. ARPE-19 cells were incubated for another 10 min, 1 h, 3 h or 12 h. Then culture medium was drawn out. ARPE-19 cells were fixed and stained using the same method in Targeting property of FA/Mel@ZnO NPs to ARPE-19 cells. The coverslip was taken out and put on a microslide to be observed under a confocal laser scanning microscope.

2.11 Morphological observation of RPE

10 μL of FA/Mel@ZnO NPs (1 mg/mL) was instilled into the eye of eight weeks old female C57 mice. After dark adaptation for 24 h later, tropicamide eyedrops were used to dilate the pupils. 30 min later, mice were exposed to 400 lx blue LED light for 2 h without shut-eye. Then, retina was separated. This retina was fixed and dealt into tissue spices. TEM was used to observe uranyl acetate andlead citrate staining spices to assess the damage of microvilli of RPE cells.

In addition, another treated mice group was used to evaluate the protective efficacy of FA/Mel@ZnO NPs on RPE cellular morphology and nucleus. The fixed spices were blotted with primary antibodies against ZO-1 and β-catenin, and with a secondary anti-IgG antibody. Then, a confocal laser scanning microscope was used to observe the tissue slices.

Mice without any treatment were set as the negative

control and non-FA/Mel@ZnO NPs administrated mice treated with blue light exposure were set as positive control.

2.12 Measurement of ROS production and antioxidant system

10 μL of FA/Mel@ZnO NPs (1 mg/mL) was instilled into the eye of eight weeks old female C57mice. After dark adaptation for 24 h later, tropicamide eyedrops were used to dilate the pupils. 30 min later, mice were exposed to 400 lx blue LED light for 2 h without shut-eye. Then, retina was separated. The ROS production and the activities of MDA, GSH-PX, T-AOC were determined using corresponding assay kits according to their explanatory protocol. Mice without any treatment were set as the negative control and non-FA/Mel@ZnO NPs administrated mice treated with blue light exposure were set as positive control.

All animal experiments were performed in accordance with the Association for Research in Vision and Ophthalmology (ARVO) Statement for the Use of Animals in Ophthalmic and Vision Research and approved by the institutional research ethics committee of Tongren University.

2.13 Western blot analysis

The tissue samples were obtained using similar method of Measurement of ROS production and antioxidant system. Proteins were blotted with primary antibodies against ERK1/2, Nrf2 or GAPDH (as an internal loading control), and with a secondary anti-IgG antibody. The immunoblots were visualized by the super signal west pico chemiluminescence substrate and imaged by the VersaDoc imaging system.

2.14 Statistical analysis

One-way or two-way ANOVA test was used to determine the statistical difference. Statistical significance was accepted at $P<0.05$.

3. Results and discussions

Firstly, ZnO QDs were surface-functionalized with TEPSA to provide carboxyl groups. We used a zinc tester to quantitatively detect the content of zinc. It was found that the content of ZnO was 65.78% in weight. Then, FA and Mel were bound to the carboxyl groups via EDC/NHS reaction. Fig. 1(a) shows the FTIR spectra of COOH@ZnO QDs and FA/Mel@ZnO NPs. There is a absorption band at 1019 cm^{-1} according to the Si-O stretching vibration (Liu *et al*. 2020). The peak at 1725 cm^{-1} and 2927 cm^{-1} are respectively attributing to the stretching vibration of C=O and O-H in carboxyl groups (Rehman *et al*. 2013). These results indicate ZnO QDs have been successfully surface-functionalized with carboxyl groups. The appearance of adsorption peak at 3302 cm^{-1} in FTIR of FA/Mel@ZnO NPs belongs to N-H stretching vibration (Huang *et al*. 2014). The peak at 1227 cm^{-1} should be attributed to =C-O-C, which is the molecular group in Mel (Uthaiwat *et al*. 2021). Besides, the band of 795 cm^{-1} and 1482 cm^{-1} are resulted from the introduction of pyridine rings of which molecular structure in FA (Bourassa and Tajmir-Riahi 2015). All the results demonstrate that the FA/Mel@ZnO NPs have been successfully synthesized. And the color of the powder turned from white to yellow due to the introduction of FA (Fig. S1). That is the accordant result. The morphology of ZnO QDs and FA/Mel@ZnO NPs were observed by TEM (Fig. 1(b)). Both of ZnO QDs and FA/Mel@ZnO NPs are monodispersed and with a homogeneous size distribution. Although the size of FA/Mel@ZnO NPs are seemingly bigger due to surface modification, their diameter ranges in 4-6 nm. This can be the suitable size allowing the NPs to easily go through the paracellular pathway to reach RPE (Horibe *et al*. 1997). In addition, we determined the zeta potentials of ZnO QDs and FA/Mel@ZnO NPs. The potential of FA/Mel@ZnO NPs turns to negative after surface modification due to the introduction of numerous carboxyl groups (Fig. 1(c)). The negative surface enables FA/Mel@ZnO NPs to escape mucoadhesion from the negatively charged corneal surface, which is convenient for FA/Mel@ZnO NPs to arrive at the posterior segment of eye (Said *et al*. 2021, Mohsen *et al*. 2020, Warsi 2021). On the other hand, positively charged DDS can adhere to negative mucin on the corneal surface. And they are suitable for delivering drug to anterior segment (Ahmed *et al*. 2021, Dubashynskaya *et al*. 2020). Next, we used TA to measure the weight of drug components in FA/Mel@ZnO NPs. As shown in Fig. 1(d), there are two obvious weight-lost segments respectively corresponding to Mel and FA. It was calculated that FA/Mel@ZnO NPs were composed of 48.36% of Mel, 20.93% of ZnO, and 13.29% of FA.

To ensure the safe dose of FA/Mel@ZnO NPs, we determined their cytotoxicity on ARPE-19 cells at the concentration ranging from 0 to 100 μM. After treatment for 24 h, the cellular viability in all experimental groups is above 97% (Fig. S2). This result confirms that FA/Mel@ZnO NPs have no toxicity on ARPE-19 cells within such concentration range and they can be the safe doses (Huang *et al*. 2020).

Ocular posterior segment is still the difficult target for drug delivery especially for administration via eyedrops (Tambe *et al*. 2021, Wang *et al*. 2021). While topical administration is always the preferred option because it is a self-administrable and non-invasive approach. And this dilemma becomes the task our FA/Mel@ZnO NPs need to accomplish. Therefore, the preliminary delivery experiment that FA/Mel@ZnO NPs permeating to posterior segment was carried out in the eyes of mouse. The distribution of FA/Mel@ZnO NPs around retina was observed by a fluorescent microscope. Even if FA/Mel@ZnO NPs reach the posterior segment, there remains another challenge that whether can they bind to RPE cells. The targeting ability to ARPE-19 cells of FA/Mel@ZnO NPs was evaluated in vitro. ZnO QDs and FA/Mel@ZnO NPs were co-cultured with ARPE-19 cells for 10 min, respectively. And cells were vigorously washed with PBS, followed by staining and observed under a confocal laser scanning microscope. The results of delivery and targeting properties of FA/Mel@ZnO

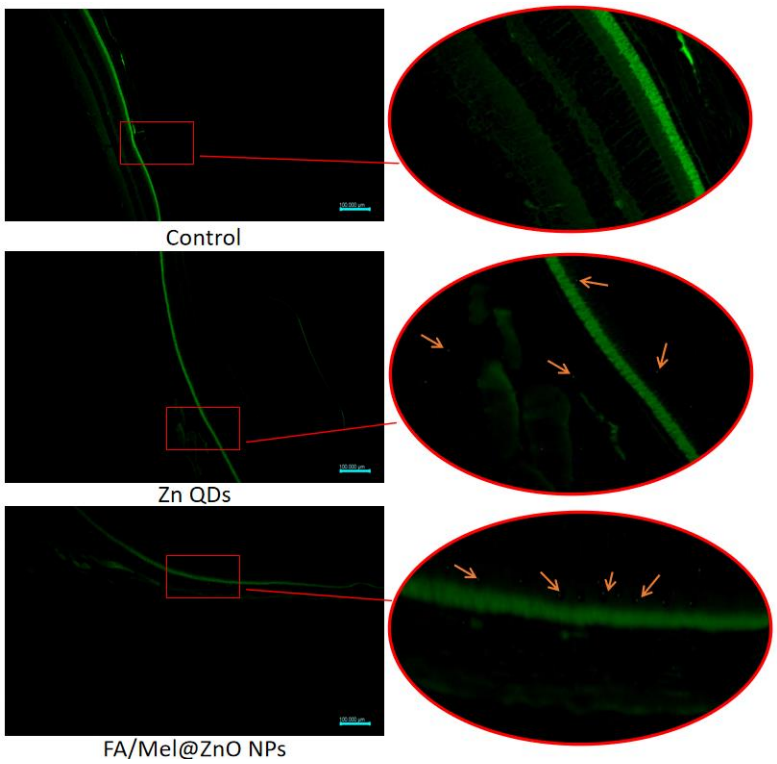

(a)

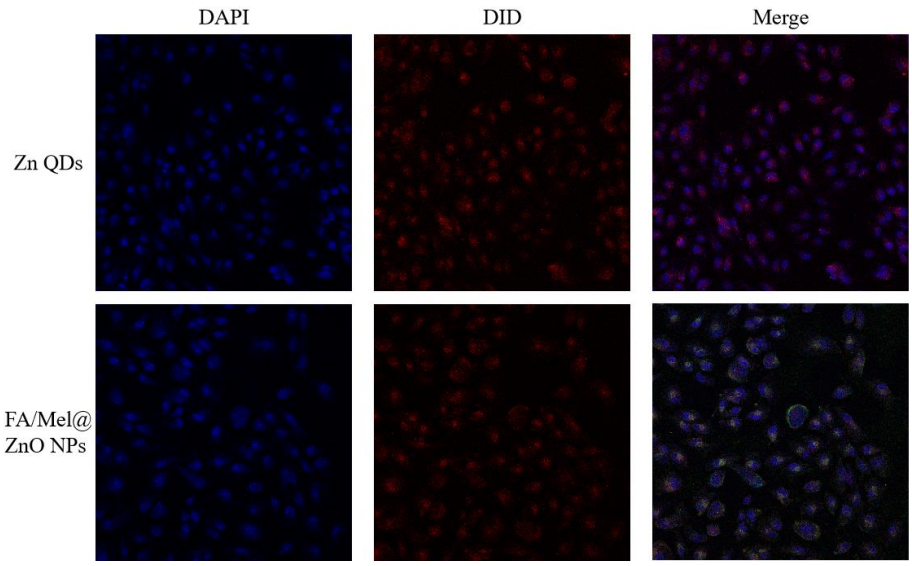

(b)

Fig. 2 The delivery behavior to retina (a) and targeting of FA/Mel@ZnO NPs to RPE cells (b)

NPs are shown in Fig. 2. It is known that ZnO can show green fluorescence after being excited (Eixenberger *et al.* 2019). 10 min after topical instillation, some fluorescence dots distributed in the surface of RPE in FA/Mel@ZnO NPs treated group. While, some fluorescence dots appeared inside RPE in ZnO QDs treated group (Fig. 2(a)). It indicates that ZnO QDs and FA/Mel@ZnO NPs are easy to reach the posterior segment, and FA/Mel@ZnO NPs retain on the surface of RPE. Moreover, as shown in Fig. 2(b), no green fluorescence can be seen around ARPE-19 cells treated with ZnO QDs and only cells treated with FA/Mel@ZnO NPs emit green fluorescence. Therefore, the results confirm that FA/Mel@ZnO NPs can specifically bind to ARPE-19 cells who express folate-receptors on the cell membrane (Suen and Chau 2013). Heretofore, few nanostructured vehicles have been developed for posterior segment drug delivery via topical administration. Yadav *et al.* (2020) found that solid lipid nanoparticles with the size around 237 nm were distributed in rat cornea, sclera, vitreous, choroid and retina after a single-drop instillation. Such nanoparticles could reach the posterior segment through corneal and conjunctival pathway due to their charge-free surface and small size. Ge *et al.* (2020) used a penetratin modified lutein-loaded nanoemulsion gel to treat

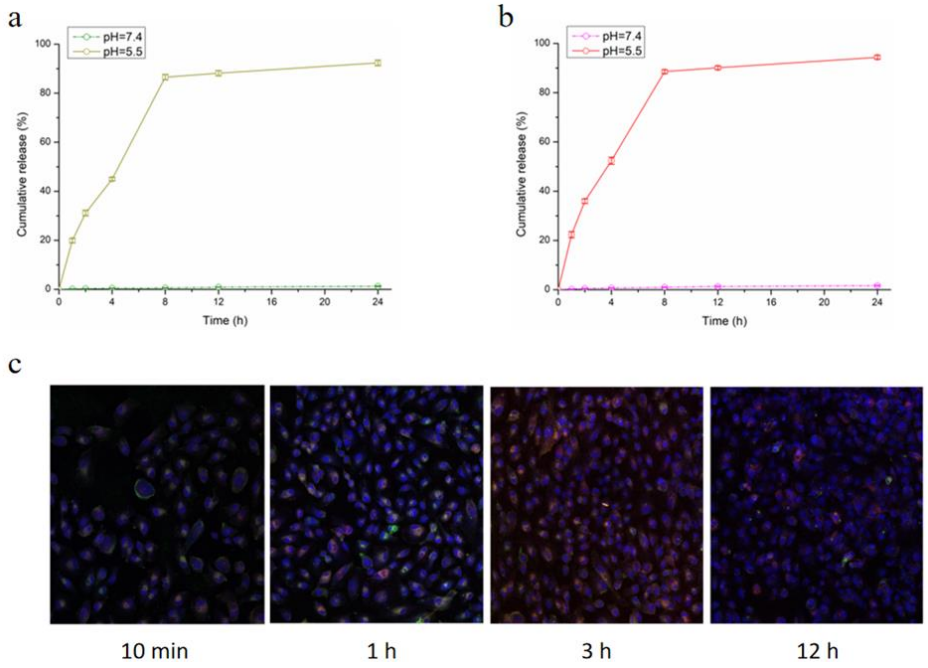

Fig. 3 The drug release behavior in vitro (a Mel; b Zn) and cellular uptake behavior of FA/Mel@ZnO NPs by ARPE-19

age-related macular degeneration via conjunctival sac instillation. They found penetratin could significantly improve the transportation of the nanoemulsion in eyes and deliver drug to fundus. Chitosan-coated liposomes also exhibited a potential permeation to the posterior segment. However, there still resided a mass of liposomes in the anterior segment (Li *et al.* 2019). The intraocular distribution of liposomes is size-dependent (Lajunen *et al.* 2014). In fact, smaller size nanocarriers (such as dendrimers with the size around 15 nm) are easier to penetrate the conjunctiva and corneal barrier to carry drugs to retina (Yang *et al.* 2019). Overall, the prerequisites of posterior segment nanocarriers are of negative-charged surface to avoid adhesion by mucin and of small size to cross the ocular barriers. Previously, all the reported vehicles are made from macromolecular materials.

Indeed, inorganic nanoparticles have potential advantages in posterior segment drug delivery. The size and distribution of inorganic nanoparticles are controllable, and inorganic nanoparticles are easy to surface-modified. So, we take the lead in using inorganic nanoparticles as the posterior segment DDS. As expected, negative and small FA/Mel@ ZnO NPs easily crossed the barrier to reach RPE with a good retention by folate receptor targeting.

Another key purpose of the prepared FA/Mel@ZnO NPs is to realize controlled release of two drugs procedurally in cells. So, we investigated the drug release behavior of FA/Mel@ZnO NPs in neutral and acidic buffer solution in vitro, respectively. The results are shown in Figs. 3(a) and 3(b). In neutral buffer solution (pH=7.4), nearly no Mel and Zn released after 24 h. Contrastively, Mel and Zn released fast in acidic buffer solution (pH=5.5). 86.56±1.12% of Mel and 88.55±0.72% of Zn released at 8 h. The release of Mel followed the release of Zn because Mel could only escape from FA/Mel@ZnO NPs after Zn QDs dissolved to Zn^{2+}. These results confirmed the pH-responsive drugs release behavior of FA/Mel@ZnO NPs. Moreover, Mel and Zn can release at the same time. Then, the cellular uptake behavior of FA/Mel@ZnO NPs (Fig. 3(c)) was observed to estimate the potential in intracellular drugs release. FA/Mel@ZnO NPs can rapidly bind to the surface of ARPE-19 cells within 10 min. After 1 h, the green fluorescence started to migrate into ARPE-19 cells, indicating the occurrence of endocytosis. At the time point of 3 h, the intensity of intracellular green fluorescence obviously heightened, displaying the enhancement of endocytosis. 9 h later, the fluorescence intensity decreased which was attributed to their acid degradation. In consideration of acid degradation of acid degradation in ARPE-19 cells, we believe that FA/Mel@ZnO NPs in cells have the same drugs release behavior as in vitro. The combination therapy can be achieved by the released Zn and Mel. pH-responsive nanocarriers is regarded as the most suitable delivery system for intracellular drug delivery owning to the acidic environment of endosome (Kanamala *et al.* 2016). Our FA/Mel@ZnO NPs are designed for targeting ARPE-19 intracellular drug delivery. They were found to reliably enter APRE-19 cells and degrade to Mel and Zn in a short time. Thus, compared to other DDS, the most attractive advantage of FA/Mel@ZnO NPs is all of the degradation products are therapeutic drugs to enhance the therapeutic effect. They are the real sense of DSDS that need no additional non-therapeutic carrier material to result in side effect. Although few pure DSDS have been reported at present (Zhao *et al.* 2020), we believe that they will be extremely beneficial to disease treatment.

RPE cells locates on the Brush membrane. Abundant melanin granules scatter in RPE cells and plentiful microvillus were at the top of RPE cells for normal mice (Fig. 4(a)). While a number of melanin granules disappeared,

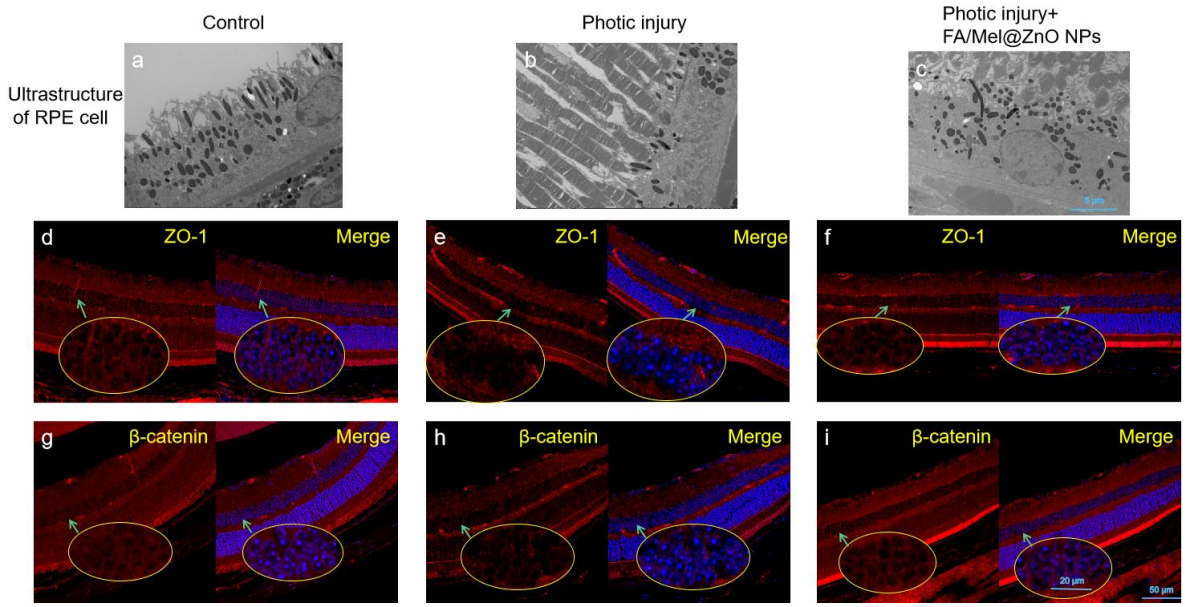

Fig. 4 The protective effect of FA/Mel@ZnO NPs (a, b, c) on ultrastructure of RPE cells and their influence on the expression of ZO-1 (d, e, f) and β-catenin (g, h, i)

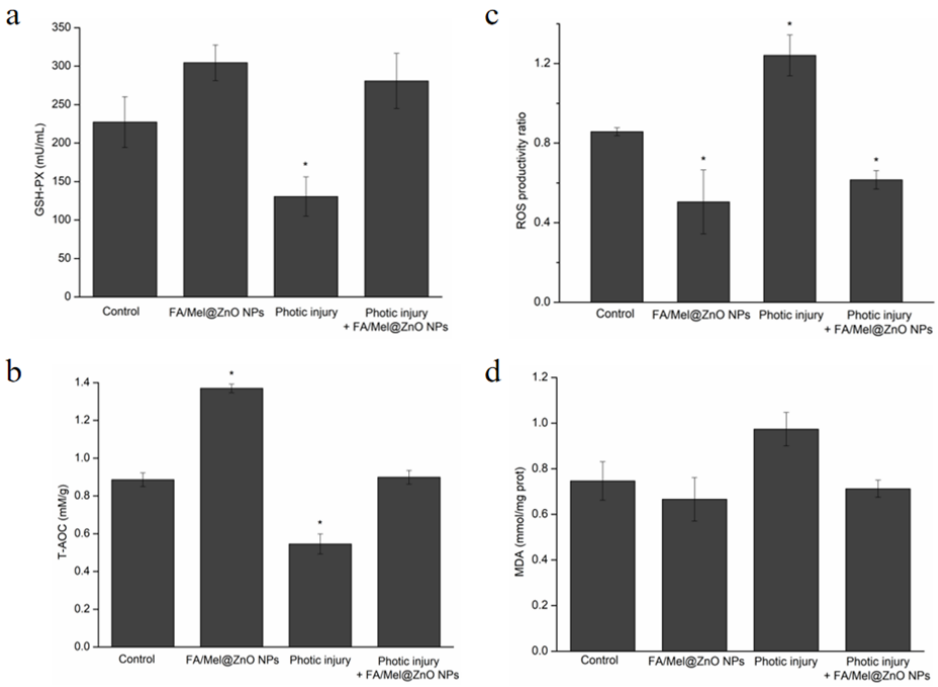

Fig. 5 The antioxidant capacity (a GSH-PX; b T-AOC; c ROS level; d MDA) of FA/Mel@ZnO NPs. ($p<0.05$, compared to the control)

and the tissue organization changed after blue light radiation (Fig. 4(b)). In Fig. 4(c), we can see that although the structure of microvillus changed a little, the amount of melanin granules is near to that of normal mice, indicating the protective effect of FA/Mel@ZnO NPs on the ultrastructure of RPE cells. Moreover, the red fluorescence signal which corresponds to the expression of ZO-1 and β-catenin significantly reduced in RPE (Figs. 4(e) and 4(h)) after blue light radiation compared to the controls (Figs. 4(d) and (g)). Whereas, the expression of ZO-1 and β-catenin did not significantly reduce under circumstance of FA/Mel@ZnO NPs dropping into the eyes of the mice before exposure to blue light. It is known that ZO-1 plays an important role on cellular mechanical barrier and permeability (Song *et al.* 2019). And β-catenin works on stabilizing intercellular adhesion (Mao *et al.* 2021). Both of them have considerable importance in maintaining the stability of cell. Therefore, our results confirm that FA/Mel@ZnO NPs can stable the structure of cell avoiding photic injury.

In order to confirm the protective effect of FA/Mel@ZnO NPs on antioxidation for RPE, we determined

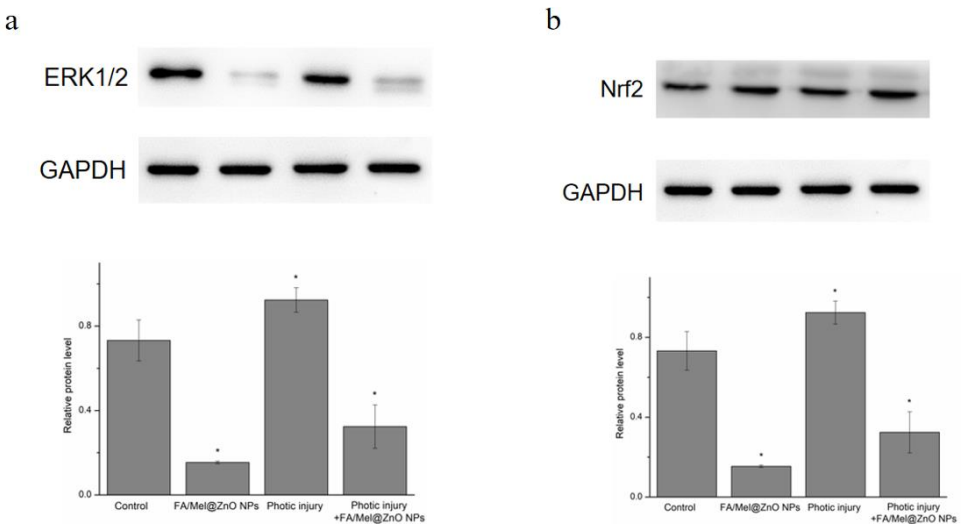

Fig. 6. Western blotting and relative protein level of ERK1/2 (a) and Nrf2 (b). (*p<0.05 compared to blank control.)

the antioxidant capacity on RPE. After topical instillation in the eyes of C57 mouse, FA/Mel@ZnO NPs could increase the GSH-PX activity (Fig. 5(a)) and T-AOC content significantly (Fig. 5(b)) of RPE, thereby decreasing the production of ROS (Fig. 5(c)) and MDA (Fig. 5(d)). Moreover, we investigated the protective effect of FA /Mel@ZnO NPs on blue-light induced oxidative stress mouse. The results show that FA/Mel@ZnO NPs obviously inhibited the production of ROS. The content of MDA, T-AOC and activity of GSH-PX in FA/Mel@ZnO NPs treated experimental groups were close to that in control groups. All the results indicate that FA/Mel@ZnO NPs can enhance antioxidation for RPE both for health mice and photic injury mice. The ROS production is more easily induced by blue light irradiation than other visible light, which is harmful to retina (Kim *et al*. 2020). When retina is exposed to blue light, it is likely to result in oxidative stress and inflammatory response to damage RPE cells. More seriously for patients, if the oxidative stress isn't regulated, some retinal diseases (such as age-related macular degeneration) eventually leading to blindness would occur (Dieguez *et al*. 2020). In view of the protective effect of FA/Mel@ZnO NPs against oxidative stress both in health mice and photic injury mice, we can infer that FA/ Mel@ZnO NPs have great potential both in prevention and treatment of oxidative damage induced retinal diseases.

We also sketchily explored the mechanism of anti-oxidant effect of FA/Mel@ZnO NPs. The expression of ERK1/2 and Nrf2 proteins were investigated. The significant decreasing trend was found in ERK1/2 level both for FA/Mel@ZnO NPs treated health mice and photic injury mice (Fig. 6(a)). ERK1/2 can be activated by some certain stressors (such as ROS). Activated ERK1/2 reduces the mitochondrial function when cells are damaged (Zhao *et al*. 2021). FA/Mel@ZnO NPs can inhibit the expression of ERK1/2, which is helpful in maintaining mitochondrial homeostasis and function. Meanwhile, the expression of Nrf2 level was up-regulated both in health mice and photic injury mice groups treated with FA/Mel@ZnO NPs (Fig. 6(b)). In the antioxidative stress signaling pathway, Nrf2 is the upstream core protein. The overall antioxidant capacity will be enhanced with the expression of Nrf2 increasing (Sekine and Motohashi 2021). FA/Mel@ZnO NPs down-regulate the ERK1/2 and up-regulate the Nrf2 signaling pathway of RPE cells to enhance the antioxidant capacity.

4. Conclusions

In conclusion, FA and Mel have successfully grafted on the surface of ZnO QDs to fabricate a new kind of drug self-delivery systems. These DSDS can easily and precisely deliver drugs to RPE via eyedrops. And they realized acid degradation to controlled release of Mel and Zn in RPE cells responding to the pH change in endosome. Consequently, the structure of RPE cells were stabilized according to the expression of ZO-1 and β-catenin. Moreover, the antioxidant capacity of RPE were enhanced both in health mice and photic injury mice, because FA/Mel@ZnO NPs probably down-regulate the ERK1/2 and up-regulate the Nrf2 signaling pathway of RPE cells. In view of their charming delivery performance to RPE and strengthened therapeutic effect, as well as their good biocompatibility, FA/Mel@ZnO NPs have great potential both in prevention and treatment of oxidative damage induced retinal diseases.

Acknowledgments

The research described in this paper was financially supported by the National Natural Science Foundation of China (No. 31800839), Growth Project of Youth Science and Technology Talent of Guizhou Education Committee (No. KY2022069) and High-level Innovative Talents in Guizhou Province (No. 2018-2016-023).

References

Ahmed, T.A., Alzahrani, M.M., Sirwi, A. and Alhakamy, N.A. (2021), "Study the antifungal and ocular permeation of ketoconazole from ophthalmic formulations containing trans-

ethosomes nanoparticles", *Pharmaceutics*, **13**(2), 151. https://doi.org/10.3390/pharmaceutics13020151.

Alvarez-Barrios, A., Alvarez, L., Garcia, M., Artime, E., Pereiro, R. and Gonzalez-lglesias, H. (2021), "Antioxidant defenses in the human eye: A focus on metallothioneins", *Antioxidants*, **10**(1), 89. https://doi.org/10.3390/antiox10010089.

Baumal, C.R., Spaide, R.F., Vajzovic, L., Freund, K.B., Walter, S.D., John, V., Rich, R., Chaudhry, N, Lakhanpal, R.R and Oellers, P.R. (2020), "Retinal vasculitis and intraocular inflammation after intravitreal injection of brolucizumab", *Ophthalmology*, **127**(10), 1345-1359. https://doi.org/10.1016/j.ophtha.2020.04.017.

Bourassa, P. and Tajmir-Riahi, H.A. (2015), "Folic acid binds DNA and RNA at different locations", *Int. J. Biol. Macromol*., **74**, 337-342. https://doi.org/10.1016/j.ijbiomac.2014.12.007.

Chang, C.C., Huang, T.Y., Chen, H.Y., Huang, T.C., Lin, L.C, Chang, Y.J. and Hsia S.M. (2018), "Protective effect of melatonin against oxidative stress-induced apoptosis and enhanced autophagy in human retinal pigment epithelium cells", *Oxid. Med. Cell. Longev*., **2018**, 9015765. https://doi.org/10.1155/2018/9015765.

Dieguez, H.H., Fleitas, M.F.G., Aranda, M.L., Calanni, J.S., Sarmiento, M.I.K., Chianelli M.S., Alaimo, A., Sande, P.H., Romeo, H.E. Rosenstein, R.E. and Dorfman, D. (2020), "Melatonin protects the retina from experimental nonexudative age-related macular degeneration in mice", *J. Pineal Res*., **68**(4), e12643. https://doi.org/10.1111/jpi.12643.

Dubashynskaya, N.V., Golovkin, A.S., Kudryavtsev, I.V., Prikhodko, S.S., Trulioff, A.S., Bokatyi, A.N., Poshina, D.N., Raik, S.V. and Skorik, V.A. (2020), "Mucoadhesive cholesterol-chitosan self-assembled particles for topical ocular delivery of dexamethasone", *Int. J. Biol. Macromol*., **158**, 811-818. https://doi.org/10.1016/j.ijbiomac.2020.04.251.

Eixenberger, J.E., Anders, C.B., Wada, K., Reddy, K.M., Brown, R.J., Moreno-Ramirez J., Weltner, A.E., Karthik, C., Tenne, D.A. and Fologea, D. (2019), "Defect engineering of ZnO nanoparticles for bioimaging applications", *ACS Appl. Mater. Inter*., **11**(28), 24933-24944. https://doi.org/10.1021/acsami.9b01582.

Ge, Y., Zhang, A., Sun, R., Xu, J., Yin, T., He, H., Gou, J., Kong, J., Zhang, Y. and Tang, X. (2020), "Penetratin modified lutein nanoemulsion in-situ gel for the treatment of age-related macular degeneration", *Expert Opin. Drug Del*., **17**(4), 603-619. https://doi.org/10.1080/17425247.2020.1735348.

Horibe, Y., Hosoya, K., Kim, K.J., Ogiso, T. and Lee, V.H.L. (1997), "Polar solute transport across the pigmented rabbit conjunctiva: Size dependence and the influence of 8-bromo cyclic adenosine monophosphate", *Pharm. Res.*, **14**(9), 1246-1251. https://doi.org/10.1023/A:1012123411343.

Huang, X., Chen, C., Zhu, X., Zheng, X., Li, S., Gong, X., Xiao, Z., Jiang, N., Yu, C. and Yi, C. (2019), "Transdermal BQ-788/EA@ZnO quantum dots as targeting and smart tyrosinase inhibitors in melanocytes", *Mater. Sci. Eng. C*, **102**, 45-52. https://doi.org/ 10.1016/j.msec.2019.04.042.

Huang, X., Wang, W., Zheng, X., Zhang, X. and Wang, Z. (2020), "Magnesium trisilicate coated Fe_3O_4 nanoparticles as prompt and efficient lactic acid removers potential for exercise-induce fatigue prevention", *J. Biomed. Nanotechnol*., **16**(4), 531-537. https://doi.org/10.1166/jbn.2020.2903.

Huang, X., Yi, C., Fan, Y., Zhang, Y., Zhao, L., Liang, Z. and Pan, J. (2014), "Magnetic Fe_3O_4 nanoparticles grafted with single-chain antibody (scFv) and docetaxel loaded beta-cyclodextrin potential for ovarian cancer dual-targeting therapy", *Mater. Sci. Eng. C*, **42**, 325-332. https://doi.org/10.1016/j.msec.2014.05.041.

Huang, X., Zheng, X., Xu, Z. and Yi, C. (2017), "ZnO-based nanocarriers for drug delivery application: From passive to smart strategies", *Int. J. Pharm*., **534**(1-2), 190-194. https://doi.org/10.1016/j.ijpharm.2017.10.008.

Ilinskaya, A.N., Clogston, J.D., McNeil, S.E. and Dobrovolskaia M.A. (2015), "Induction of oxidative stress by Taxol (R) vehicle Cremophor-EL triggers production of interleukin-8 by peripheral blood mononuclear cells through the mechanism not requiring de novo synthesis of mRNA", *Nanomed. Nanotechnol*., **11**(8), 1925-1938. https://doi.org/10.1016/j.nano.2015.07.012.

Kim, J., Cho, K. and Choung, S.Y. (2020), "Protective effect of Prunella vulgaris var. L extract against blue light induced damages in ARPE-19 cells and mouse retina", *Free Radical Bio. Med*., **152**, 622-631. https://doi.org/10.1016/j.freeradbiomed.2019.12.003.

Lajunen, T., Hisazumi, K., Kanazawa, T., Okada, H., Seta, Y., Yliperttula, M., Urtti, A. and Takashima, Y. (2014), "Topical drug delivery to retinal pigment epithelium with microfluidizer produced small liposomes", *Eur. J. Pharm. Sci*., **62**, 23-32. https://doi.org/10.1016/j.ejps.2014.04.018.

Li, J., Cheng, T., Tian, Q., Cheng, Y., Zhao, L., Zhang, X. and Qu, Y. (2019), "A more efficient ocular delivery system of triamcinolone acetonide as eye drop to the posterior segment of the eye", *Drug Deliv*., **26**(1), 188-198. https://doi.org/ 10.1080/10717544.2019.1571122.

Liu, X., Jiang, J. and Meng, H. (2019), "Transcytosis-An effective targeting strategy that is complementary to "EPR effect" for pancreatic cancer nano drug delivery", *Theranostics*, **9**(26), 8018-8025. https://doi.org/10.7150/thno.38587.

Liu, Y., Zeng, F., Sun, B. and Jia, P. (2020), "Research on XRD and FTIR spectra of fly ash in different particle size from Gujiao power plant", *Spectrosc. Spect. Anal*., **40**(5), 1452-1456. https://doi.org/ 10.3964/j.issn.1000-0593(2020)05-1452-05.

Mao, L., Yang, J., Yue, J., Chen, Y., Zhou, H., Fan, D., Zhang, Q., Buraschi, S., Iozzo, R.V. and Bi, X. (2021), "Decorin deficiency promotes epithelial-mesenchymal transition and colon cancer metastasis", *Matrix Biol*., **95**, 1-14. https://doi.org/10.1016/j.matbio.2020.10.001.

Mehrzadi, S., Hemati, K., Reiter, R.J. and Hosseinzadeh, A. (2020), "Mitochondrial dysfunction in age-related macular degeneration: melatonin as a potential treatment", *Expert Opi. Ther. Tar*., **24**(4), 359-378. https://doi.org/10.1080/14728222.2020.1737015.

Mohsen, A.M., Salama, A. and Kassem, A.A. (2020), "Development of acetazolamide loaded bilosomes for improved ocular delivery: Preparation, characterization and in vivo evaluation", *J. Drug Deliv. Sci. Tec*., **59**, 101910. https://doi.org/10.1016/j.jddst.2020.101910.

Mu, W., Chu, Q., Liu, Y. and Zhang, N. (2020), "A review on nano-based drug delivery system for cancer chemoimmuno-therapy", *Nano-Micro Lett*., **12**(1), 142. https://doi.org/10.1007/s40820-020-00482-6.

Piscatelli, J.A., Ban, J., Lucas, A.T. and Zamboni, W.C. (2021), "Complex factors and challenges that affect the pharmacology, safety and efficacy of nanocarrier drug delivery systems", *Pharmaceutics*, **13**(1), 114. https://doi.org/10.3390/pharmaceutics13010114.

Qin, S.Y., Zhang, A.Q., Cheng, S.X., Rong, L. and Zhang, X.Z. (2017), "Drug self-delivery systems for cancer therapy", *Biomaterials*, **112**, 234-247. https://doi.org/10.1016/j.biomaterials.2016.10.016.

Rehman A.U., Abbas, S.M., Ammad, H.M., Badshah, A., Ali, Z. and Anjum, D.H. (2013), "A facile and novel approach towards carboxylic acid functionalization of multiwalled carbon nanotubes and efficient water dispersion", *Mater. Lett*., **108**, 253-256. https://doi.org/10.1016/j.matlet.2013.07.009.

Rodriguez-Menendez, S., Garcia, M., Fernandez, B., Alvarez, L., Fernandez-Vega-Cueto, A., Coca-Prados, M., Pereiro, R. and

Gonzalez-lglesias H. (2018), "The zinc-metallothionein redox system reduces oxidative stress in retinal pigment epithelial cells", *Nutrients*, **10**(12), 1874. https://doi.org/10.3390/nu10121874.

Rzhanova, L.A., Kuznetsova, A.V. and Aleksandrova, M.A. (2020), "Reprogramming of differentiated mammalian and human retinal pigment epithelium: current achievements and prospects", *Russ. J. Dev. Biol.*, **51**(4), 212-230. https://doi.org/10.1134/S1062360420040062.

Said, M., Aboelwafa, A.A., Elshafeey, A.H. and Elsayed, I. (2021), "Central composite optimization of ocular mucoadhesive cubosomes for enhanced bioavailability and controlled delivery of voriconazole", *J. Drug Deliv. Sci. Tec.*, **61**, 102075. https://doi.org/10.1016/10.1016/j.jddst.2020.102075.

Saito, Y., Kuse, Y., Inoue, Y., Nakamura, S., Hara, H. and Shimazawa, M. (2018), "Transient acceleration of autophagic degradation by pharmacological Nrf2 activation is important for retinal pigment epithelium cell survival", *Redox Biol.*, **19**, 354-363. https://doi.org/10.1016/j.redox.2018.09.004.

Sekine, H. and Motohashi, H. (2021), "Roles of CNC transcription factors NRF1 and NRF2 in cancer", *Cancers*, **13**(3), 541. https://doi.org/10.3390/cancers13030541.

Shen, J., Wolfram, J., Ferrari, M. and Shen, H. (2017), "Taking the vehicle out of drug delivery", *Mater. Today*, **20**(3), 95-97. https://doi.org/10.1016/j.mattod.2017.01.013.

Singh, T.A., Das, J. and Sil, P.C. (2020), "Zinc oxide nanoparticles: A comprehensive review on its synthesis, anticancer and drug delivery applications as well as health risks", *Adv. Colloid Interfac.*, **286**, 102317. https://doi.org/ 10.1016/j.cis.2020.102317.

Song, H., Zheng, J., He, W., Wang, P. and Wang, F. (2019), "Activation of cofilin increases intestinal permeability via depolymerization of F-actin during hypoxia in vitro", *Front. Physiol.*, **10**, 1455. https://doi.org/10.3389/fphys.2019.01455.

Subrizi, A, del Amo, E.M., Korzhikov-Vlakh, V., Tennikova, T., Ruponen, M. and Urtti, A. (2019), "Design principles of ocular drug delivery systems: importance of drug payload, release rate, and material properties", *Drug Discov. Today*, **24**(8), 1446-1457. https://doi.org/10.1016/j.drudis.2019.02.001

Suen, W.L.L. and Chau, Y. (2013), "Specific uptake of folate-decorated triamcinolone-encapsulating nanoparticles by retinal pigment epithelium cells enhances and prolongs antiangiogenic activity", *J. Control. Release*, **167** (1), 21-28. https://doi.org/10.1016/j.jconrel.2013.01.004.

Tambe, V., Raval, N., Gondaliya, P., Bhattacharya, P., Kalia, K. and Tekade, R.K. (2021), "To investigate fit-to-purpose nanocarrier for non-invasive drug delivery to posterior segment of eye", *J. Drug Deliv. Sci. Tec.*, **61**, 102222. https://doi.org/10.1016/j.jddst.2020.102222.

Uthaiwat, P., Priprem, A., Puthongking, P., Daduang, J., Nukulkit, C., Chio-Srichan, S., Boonsiri, P. and Thapphasaraphong, S. (2021), "Characteristic evaluation of gel formulation containing niosomes of melatonin or its derivative and mucoadhesive properties using ATR-FTIR spectroscopy", *Polymers*, **13**(7), 1142. https://doi.org/10.3390/polym13071142.

Wang, R., Gao, Y., Liu, A. and Zhai, G. (2021), "A review of nanocarrier-mediated drug delivery systems for posterior segment eye disease: challenges analysis and recent advances", *J. Drug Target.*, **29**(7), 687-702. https://doi.org/10.1080/1061186X.2021.1878366.

Warsi, M.H. (2021), "Development and optimization of vitamin E TPGS based PLGA nanoparticles for improved and safe ocular delivery of ketorolac", *J. Drug Deliv. Sci. Tec.*, **61**, 102121. https://doi.org/10.1016/j.jddst.2020.102121.

Wilhelm, S., Tavares, A.J., Dai, Q., Qhta, S., Audet, J., Dvorak, H.F. and Chan, W.C.W. (2016), "Analysis of nanoparticle delivery to tumours", *Nat. Rev. Mater.*, **1**(5), 16014. https://doi.org/10.1038/natrevmats.2016.14.

Yadav, M., Schiavone, N., Guzman-Aranguez, A., Giansanti, F., Papucci, L., de Lara, M.J.P., Singh, M. and Kaur, I.P. (2020), "Atorvastatin-loaded solid lipid nanoparticles as eye drops: proposed treatment option for age-related macular degeneration (AMD)", *Drug Deliv. Transl. Res.*, **10**(4), 919-944. https://doi.org/10.1007/s13346-020-00733-4.

Yang, X., Wang, L., Li, L., Han, M., Tang, S., Wang, T., Han, J., He, X., He, X., Wang, A. and Sun, K. (2019), "A novel dendrimer-based complex co-modified with cyclic RGD hexapeptide and penetratin for noninvasive targeting and penetration of the ocular posterior segment", *Drug Deliv.*, **26**(1), 989-1001. https://doi.org/10.1080/10717544.2019.1667455.

Yu, K., Liu, M., Dai, H. and Huang, X. (2020), "Targeted drug delivery systems for bladder cancer therapy", *J. Drug Deliv. Sci. Tech.*, **56**, 101535. https://doi.org/10.1016/j.jddst.2020.101535.

Zhao, L.P., Zheng, R.R., Huang, J.Q., Chen, X.Y., Deng, F.A., Liu, Y.B., Huang, C.Y., Yu, X.Y., Cheng, H. and Li, S.Y. (2020), "Self-delivery photo-immune stimulators for photo-dynamic sensitized tumor immunotherapy", *ACS Nano*, **14**(12), 17100-17113. https://doi.org/10.1021/acsnano.0c06765.

Zhao, Y., Gao, J., Zhang, Y., Gan, X. and Yu, H. (2021), "Cyclosporine a promotes bone remodeling in LPS-related inflammation via inhibiting ROS/ERK signaling: Studies In vivo and in vitro", *Oxid. Med. Cell. Longev.*, 8836599. https://doi.org/10.1155/2021/8836599.

CC

Appendix

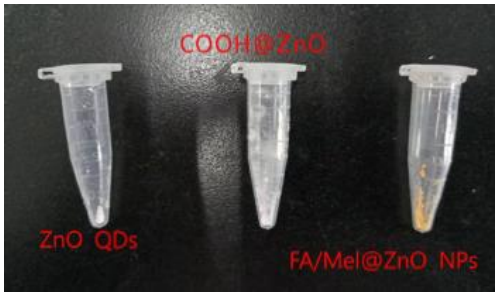

Fig. S1 The photographs of ZnO QDs, COOH@ZnO QDs and FA/Mel@ZnO NPs

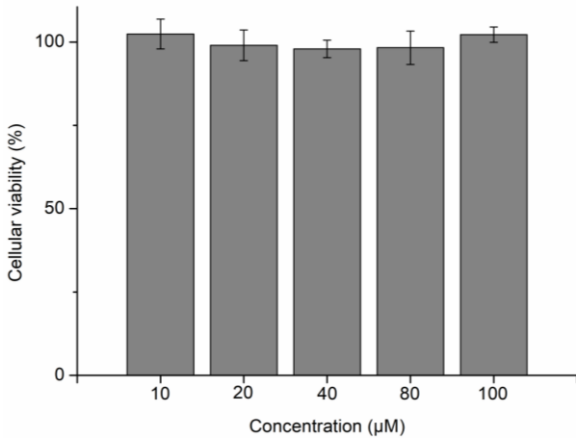

Fig. S2 The cytotoxicity of FA/Mel@ZnO NPs on ARPE-19 cells